

International Journal of Modern Physics A
 © World Scientific Publishing Company

SUPERSYMMETRY AT AND BEYOND THE LHC

JAN KALINOWSKI

*Institute of Theoretical Physics, University of Warsaw
 Hoza 69, 00681 Warsaw, Poland
 jan.kalinowski@fuw.edu.pl*

Received Day Month Year

Revised Day Month Year

Prospects for SUSY discoveries and measurements at future colliders LHC and ILC are discussed. The problem of reconstructing the underlying theory and SUSY breaking mechanism is also addressed.

Keywords: supersymmetry, colliders, LHC, ILC.

PACS numbers: 12.15.-y, 12.60.-i

1. Introduction

The Standard Model (SM) is very successful in describing the constituents of matter and their interactions at and below the electroweak scale¹. However, it does not address many important issues, like the mass generation and mass pattern, the unification of all forces (including gravity), the matter composition of our universe etc. These issues seem to point to new phenomena at a TeV scale which can experimentally be tested soon at the Large Hadron Collider (LHC) and in (hopefully) not too far a future at the International Linear Collider (ILC).

Although the answers to these issues could have different origin, it is very tempting to contemplate supersymmetry² (SUSY) as responsible for all of them. SUSY turned to be able to beautifully accommodate or explain (at least in the technical sense) some of the SM problems, *e.g.* it solves the hierarchy problem, explains the gauge coupling unification, provides the radiative electroweak symmetry breaking, provides a candidate for dark matter (DM), offers new ideas on matter-antimatter asymmetry of the universe *etc.* SUSY still lacks any direct experimental evidence, however, is not yet excluded either.

Discovering supersymmetry, the main candidate for a unified theory beyond the SM, is the challenge for world physics community experimenting at existing and future colliders. Many detailed phenomenological studies of SUSY at present and future colliders have been performed in the past. Here only some selected results are presented on the discovery potentials of the main two LHC detectors: ATLAS and CMS. Assuming that SUSY is discovered at LHC we will discuss how experi-

2 Jan Kalinowski

mentation at the ILC will help in revealing the details of the underlying model and address the question of reconstructing the fundamental SUSY parameters and the mechanism of SUSY breaking.

2. Supersymmetry searches at the LHC

At present the most restrictive limits on the SUSY parameter space come from negative results of SUSY searches³ at two colliders: Tevatron at Fermilab and HERA at DESY. Both machines perform beautifully and significant improvements (or discoveries) can be expected in near future until the LHC will start taking data.

The strongly interacting squarks and gluinos (\tilde{q} and \tilde{g}), if they are in the TeV range, will be copiously produced at the LHC with production cross sections comparable to jet production with transverse momenta $p_t \sim$ SUSY masses (typically in the picobarn range). Direct production of weakly interacting sparticles has much lower rates. Squarks and gluinos will promptly decay into jets and lighter SUSY particles which will further decay. Generically one can expect in the final state high- p_t jets and leptons, possibly large missing energy \cancel{E}_t , or displaced vertices *etc.* Since the LHC detectors are designed to detect these objects, they are well equipped to cover a broad spectrum of possible decay modes of SUSY particles. There have been many experimental analyses demonstrating the capabilities of the LHC detectors ATLAS and CMS and we refer to technical design reports^{4,5} of both collaboration for more details.

2.1. Inclusive searches at LHC

Jets from squark and gluino decays will have large transverse momenta p_t of the order of sparticle masses. If the lightest SUSY particle (LSP) is stable, as in scenarios with R -parity conserved, it will escape undetected giving large \cancel{E}_t . The SM background events from top quark, W and Z boson decays do not have such high- p_t objects. A set of simple cuts can then be designed to enhance the signal over the background in inclusive “transverse” searches for SUSY particles. For example, in typical mSUGRA scenarios, requiring at least four jets with large p_t^i and large

$$M_{\text{eff}} = \sum_{i=1,\dots,4} p_t^i + \cancel{E}_t \quad (1)$$

and selecting events spherical in the transverse plane (specific cuts depend on details of the model) can be sufficient to discover new particles⁴. To reduce the background further, hard, isolated lepton(s) may be required and their p_t is then included in the definition of M_{eff} . The reach of inclusive searches at 10^{-1} fb is illustrated in Fig. 1; and squarks and gluinos with masses up to ~ 2.5 TeV can be found at LHC with 100 fb^{-1} . Monte Carlo studies have also shown that the position of the peak in M_{eff} distribution correlates quite well with sparticle masses, namely $M_{\text{eff}} \sim \min(m_{\tilde{q}}, m_{\tilde{g}})$, providing a first estimate of the overall SUSY mass scale, Fig. 1 right panel.

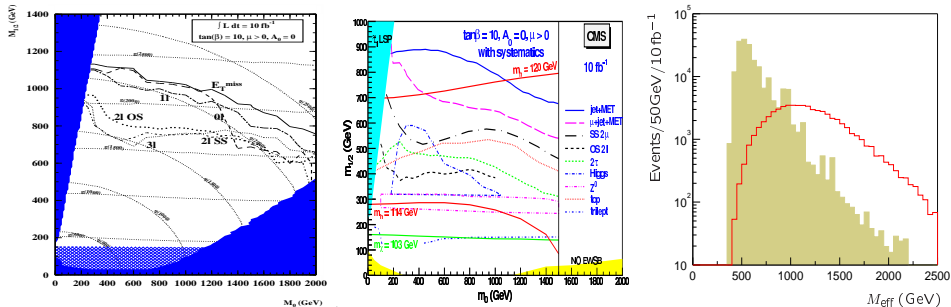


Fig. 1. Search limits for various channels in the $mSUGRA$ parameter space (left and center) and M_{eff} distribution for a $mSUGRA$ point and SM background after cuts (right).

Recently the importance of including exact matrix element corrections to the previous parton shower estimate of the background has been emphasized⁶. This may significantly change the background distribution in the signal region. This is particularly important in scenarios with sparticle masses degenerate in which the signal events are less “transverse”. As a result, the standard SUSY cuts reduce the signal sample and SUSY discovery is more affected by the SM background. Such a scenario occurs, for example, in a string inspired model based on the flux compactification⁷, in which the unification scale of the soft SUSY parameters can be much lower than the GUT scale, even of the order of the weak scale⁸. Depending on the ratio of F-terms of the volume modulus field and the mSUGRA compensator field, the mass spectrum of SUSY particles changes smoothly from the mSUGRA-like to the anomaly-mediation-like. There are regions of parameters where the squark, slepton and gaugino masses are significantly degenerated. If $m_{\tilde{\chi}_0^0} \gtrsim m_{\tilde{q}, \tilde{g}}/2$, the signal M_{eff} distribution becomes quite similar to that of the background. New ideas are needed to improve search strategies. For example, examining the pattern of events in the $M_{\text{eff}}\text{--}E_t$ plane may help to discriminate signal from background better⁹.

2.2. *Sparticle mass measurements*

In R -parity conserving SUSY all sparticles decay into invisible LSP, so no mass peaks can be directly reconstructed. Nevertheless, it might be possible to identify particular decay chains and exploit the “endpoint method” to measure combinations of masses¹⁰. A relatively clean channel, for example, is provided by the three-body decay or, if the slepton can be on-shell, the cascade of two-body decays of the heavier neutralino

$$\tilde{\chi}_i^0 \rightarrow \tilde{\ell}\ell \rightarrow \ell\ell\tilde{\chi}_1^0 \quad (2)$$

The di-lepton mass distribution endpoints are functions of the masses of particles involved in the decay

$$m_{\ell\ell}(3\text{-body}) = m_{\tilde{\chi}_i^0} - m_{\tilde{\chi}_1^0} \quad (3)$$

$$m_{\ell\ell}(2\text{-body}) = \sqrt{(m_{\tilde{\chi}_i^0}^2 - m_{\tilde{\ell}}^2)(m_{\tilde{\ell}}^2 - m_{\tilde{\chi}_1^0}^2)}/m_{\tilde{\ell}} \quad (4)$$

Requiring two isolated leptons in addition to multi-jet and \cancel{E}_t cuts, like those described above, the signal events can be selected. If lepton flavor is conserved, contributions from two uncorrelated decays cancel in the combination of $e^+e^- + \mu^+\mu^- - e^\pm\mu^\mp$ sample giving a very clean signal and allowing a precise endpoint measurement. The shape of the distribution also helps to distinguish two-body from three-body decays.

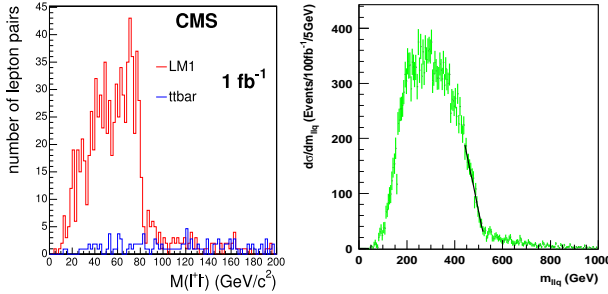


Fig. 2. Di-lepton (left) and $\ell\bar{q}$ (right) invariant mass distributions from $\tilde{\chi}_2^0$ cascade decay.

Long decay chains, like

$$\tilde{g} \rightarrow j_1 \tilde{q} \rightarrow \tilde{\chi}_2^0 j_1 j_2 \rightarrow \tilde{\ell} \ell_1 j_1 j_2 \rightarrow \tilde{\chi}_1^0 \ell_1 \ell_2 j_1 j_2 \quad (5)$$

expected in some mSUGRA scenarios *e.g.* SPS1a¹¹, allow more endpoint measurements. With two jets and two leptons in the final state it should be possible to measure the endpoints of invariant mass distributions $\ell\ell$, $\ell\bar{q}$, ℓj , like those shown in Fig. 2. Although these endpoints are smeared by jet reconstruction, hadronic resolution, and miss-assignment of the jets that come from squark decays, these endpoints should be measured at the level of 1%, *i.e.* determining mass relations to 1-2%¹². In fact, with so many endpoints one can solve for the absolute values of the unknown masses of \tilde{g} , \tilde{q} , $\tilde{\chi}_2^0$, $\tilde{\ell}$ and $\tilde{\chi}_1^0$ within 5–10% accuracy. This is a general feature of the determination of sparticle masses when the LSP momentum cannot be measured directly. For this particular point, already $\mathcal{O}(5)\%$ accuracy in the mass of sleptons and the lightest neutralino can provide a link to cosmology. Based in this information one can calculate the neutralino annihilation rate at the time of decoupling and estimate the amount of DM at the level of 7%¹³. For other scenarios, however, the expected accuracy can be much worse¹⁴.

It is notable that via the above decay chain the LHC can access the heaviest neutralino $\tilde{\chi}_4^0$ which in the SPS1a' scenario is too heavy to be produced at the 500 GeV e^+e^- collider. The measured mass difference $m_{\tilde{\chi}_4^0} - m_{\tilde{\chi}_1^0}$, in the same decay

chain as in eq.(5), but with $\tilde{\chi}_4^0$ replacing $\tilde{\chi}_2^0$, would provide an important constraint on model parameters. If the measurements at the LHC and ILC could be combined the errors for the MSSM Lagrangian parameters would significantly be reduced¹⁵.

The mass determination through the endpoint method has several shortcomings: the LSP momentum cannot be reconstructed except for a few very special points in the parameter space, only events near endpoints are used neglecting independent information contained in events away, and the selected events may contain contributions from several cascade decays causing additional systematic uncertainties. An alternative “mass relation” method¹⁶, which exploits the on-shell conditions for sparticle masses in the decay chains, allows to solve for the kinematics and reconstruct the SUSY masses as peaks in certain distributions. For example, in the cascade decay eq.(5) five on-shell conditions can be written for \tilde{g} , \tilde{q} , $\tilde{\chi}_2^0$, $\tilde{\ell}$ and $\tilde{\chi}_1^0$ in terms of the measured momenta of leptons, jets and 4 unknown momentum components of the undetected neutralino. Each event, therefore, spans a 4-dim hypersurface in a 5-dim mass space, and in principle 5 events would be enough to solve for masses of involved sparticles. Note that events need not be close to endpoints of the decay distributions, *i.e.* the method can be used even if the number of signal events is small.

2.3. Proving it is SUSY

A generic signal of large \cancel{E}_t , as in the weak-scale SUSY, arises in almost any model with the lightest $\mathcal{O}(100 \text{ GeV})$ particle stable and neutral, as suggested by the dark matter of the universe. Therefore, we have to be able to distinguish the SUSY decay chain eq.(5) from, *e.g.*, the cascade decay

$$g' \rightarrow j_1 q' \rightarrow Z' j_1 j_2 \rightarrow \ell' \ell_1 j_1 j_2 \rightarrow \gamma' \ell_1 \ell_2 j_1 j_2 \quad (6)$$

that arises in the universal extra-dimension model (UED)¹⁷. Here the primes denote the first excited Kaluza-Klein states of the corresponding SM particles. In both cases the final state is the same $\ell_1 \ell_2 j_1 j_2$ with either the $\tilde{\chi}_1^0$ or the γ' escaping detection. What differentiates the decays in eqs.(5,6) is the spins of intermediate states and the chiral structure of couplings. In contrast to the UED case, in many processes the SUSY particles are naturally polarized due to the chiral structure of the theory. For example, in the decay $\tilde{q}_L \rightarrow \tilde{\chi}_2^0 q_L$ the $\tilde{\chi}_2^0$ is polarized as right-handed, opposite to q_L , because the $\tilde{q}\tilde{\chi}q$ Yukawa coupling flips chirality. The polarized neutralino further decays into either $\tilde{\ell}_R \ell^+$ or $\tilde{\ell}_R^* \ell^-$ with equal rates (because of the Majorana character of neutralinos), but due to the chiral nature of the Yukawa $\tilde{\ell}\tilde{\chi}\ell$ coupling, the ℓ^+ is likely to fly in the neutralino direction in the squark rest frame, while the ℓ^- in the direction of the quark jet. The difference in the angular distribution is reflected as a charge asymmetry in the invariant mass distribution of the jet-lepton system¹⁸.

Although the charge asymmetry for \tilde{q}_L^* decay is just opposite, in pp collisions more squarks than anti-squarks are expected and the $\tilde{\chi}_2^0$ production from squark decays

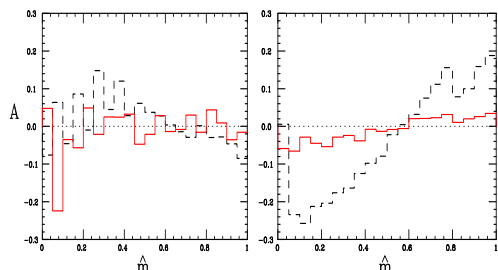


Fig. 3. Detector-level charge asymmetries with respect to the jet+lepton rescaled invariant mass, for UED- (left) and SUSY-like (right) mass spectra. Dashed: SUSY. Solid/red: UED.

is dominant. The amount of charge asymmetry in the $m(j\ell)$ is model dependent, Fig. 3, nevertheless it may allow resolving the fermionic nature of the neutralino from the vector nature of the Z' and confirm the chiral structure of couplings^{19,20}.

2.4. The LHC inverse problem

The LHC experiments in the supersymmetric particle sector offer not only the discovery potential but also many high precision measurements of masses and couplings. The next step towards establishing SUSY is the reconstruction of low-energy SUSY breaking Lagrangian parameters without assuming a specific scenario. This is a highly non-trivial task²¹. In some favorable cases it might be possible to reconstruct the model. However, in many cases one is left with degenerate solutions, *i.e.* many models could fit the LHC data equally well²².

This task can be greatly ameliorated by experimenting at the ILC where the experimental accuracies at the per-cent down to the per-mil level are expected²³.

3. SUSY studies at the ILC

If the superpartner masses (at least some of them) are in the TeV range, LHC will certainly see SUSY. Many different channels, in particular from squark and gluino decays will be explored and many interesting quantities measured, as discussed in the previous chapter. However, to achieve the ultimate goal of all experimental efforts to unravel the SUSY breaking mechanism and shed light on physics at high (GUT?, Planck?) scale, an e^+e^- LC would be an indispensable tool²³. First, the LC will provide independent checks of the LHC findings. Second, thanks to the LC unique features: clean environment, tunable collision energy, high luminosity, polarized incoming beams, and possibly e^-e^- , $e\gamma$ and $\gamma\gamma$ modes, it will offer precise measurements of masses, couplings, quantum numbers, mixing angles, CP phases etc. Last, but not least, it will provide additional experimental input to the LHC analyses, like the mass of the LSP. Coherent analyses of data from the LHC and LC would thus allow for a better, model independent reconstruction of low-energy SUSY parameters, and connect low-scale phenomenology with the high-scale physics²⁴.

An intense R&D process and physics studies since 1992 has lead to world-wide consensus that the next high energy machine after the LHC should be an International Linear Collider (ILC). Planning, designing and funding the ILC requires

global participation and global organization. Therefore the Global Design Effort for the ILC²⁵, headed by Barry Barish, has been established with the goal of preparing the project to be ready for approval around 2010 and beginning construction around 2012. Recently released the Reference Design Report²⁶ defines the ILC baseline as follows:

- CM energy adjustable from 200 to 500 GeV, and at M_Z for calibration,
- integrated luminosity of at least 500 fb^{-1} in first 4 years,
- beam energy stability and precision below 1%,
- electron beam polarization of at least 80%,
- upgradeability to CM energy of 1 TeV.

The choice of options, like GigaZ (high luminosity run at M_Z), positron polarization, e^-e^- , $e\gamma$ or $\gamma\gamma$, will depend on LHC+ILC physics results.

Many detailed physics calculations and simulations have been performed and presented during numerous ECFA, ACFA and ALCPG workshops and LCWS conferences²⁷. Below only some highlights are presented.

3.1. Mass measurements

At the ILC two methods can be used to measure particle masses: threshold scans or in continuum. The shape of the production cross section near threshold is sensitive to the masses and quantum numbers. For first 2 generations, where R - L mixing can be neglected for example, $\tilde{\mu}_L^+\tilde{\mu}_L^-$, $\tilde{\mu}_R^+\tilde{\mu}_R^-$, $\tilde{e}_L^+\tilde{e}_L^-$ and $\tilde{e}_R^+\tilde{e}_R^-$ pairs are excited in P-wave characterized by a slow rise of the cross section $\sigma \sim \beta^3$ with slepton velocity β . On the other hand, in $e_L^+e_L^-/e_R^+e_R^- \rightarrow \tilde{e}_R^+\tilde{e}_L^-/\tilde{e}_L^+\tilde{e}_R^-$ and $e_L^-e_L^-/e_R^-e_R^- \rightarrow \tilde{e}_L^-\tilde{e}_L^-/\tilde{e}_R^-\tilde{e}_R^-$ sleptons are excited in S-wave giving steep rise of the cross sections $\sigma \sim \beta$. Simulations for the SPS1a point²⁸, Fig. 4²⁹, show that the \tilde{e}_R mass can be determined to 2 per mil; the resolution deteriorates by a factor of ~ 2 for $\tilde{\mu}_R^+\tilde{\mu}_R^-$ production. For $e_R^-e_R^- \rightarrow \tilde{e}_R\tilde{e}_R$ the fast rise of the cross section allows to gain a factor ~ 4 in precision already at a tenth of the luminosity if the e^+e^- case.

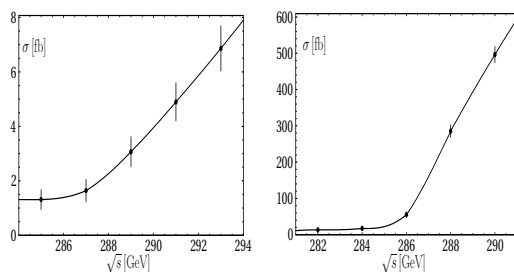


Fig. 4. Cross sections at threshold for the reactions $e_L^+e_R^- \rightarrow \tilde{e}_R^+\tilde{e}_L^-$ (left) and $e_R^-e_R^- \rightarrow \tilde{e}_R^+\tilde{e}_R^-$ (right) in the SPS1a scenario, including background. Error bars correspond to a luminosity of 10 fb^{-1} (left) and 1 fb^{-1} (right) per point.. Note different vertical scales.

Above the threshold, slepton masses can be obtained from the endpoint energies of leptons coming from slepton decays. In the case of two-body decays, $\tilde{\ell}^- \rightarrow \ell^- \tilde{\chi}_i^0$ and $\tilde{\nu}_\ell \rightarrow \ell^- \tilde{\chi}_i^+$ the lepton energy spectrum is flat with endpoints (the minimum

E_- and maximum E_+ energies) given by

$$E_{\pm} = \frac{1}{4}\sqrt{s}(1 \pm \beta)(1 - m_{\tilde{\chi}}^2/m_{\tilde{\ell}}^2) \quad (7)$$

Unlike at the LHC, the knowledge of the collision energy allows not only an accurate determination of the mass of the primary slepton but also the secondary neutralino/chargino. One finds that $m_{\tilde{e}_R}$, $m_{\tilde{\mu}_R}$ and $m_{\tilde{\chi}_1^0}$ can be measured to 0.1 to 0.18 GeV, *i.e.* 2 per mil in selectron and smuon production processes³⁰. The $\tilde{\mu}_L$ is more difficult to detect because of large background from WW pairs and SUSY cascades. However, high luminosity allows one to select the rare decay modes $\tilde{\mu}_L \rightarrow \mu \tilde{\chi}_2^0$ and $\tilde{\chi}_2^0 \rightarrow \ell^+ \ell^- \tilde{\chi}_1^0$ leading to a unique, background free signature $\mu^+ \mu^- 4\ell^{\pm} \cancel{E}$. The achievable mass resolution for $m_{\tilde{\mu}_L}$ and $m_{\tilde{\chi}_2^0}$ is of the order 4 per mil³¹.

The chargino masses can be measured very precisely at threshold: simulations for the reaction $e_R^+ e_L^- \rightarrow \tilde{\chi}_1^+ \tilde{\chi}_1^- \rightarrow \ell^{\pm} \nu_{\ell} \tilde{\chi}_1^0 q \bar{q}' \tilde{\chi}_1^0$ show that the mass resolution is excellent of $\mathcal{O}(50 \text{ MeV})$, degrading to the per mil level for the higher $\tilde{\chi}_2^{\pm}$ state. Above threshold, from the di-jet energy distribution in $\tilde{\chi}_2^{\pm} \rightarrow q \bar{q}' \tilde{\chi}_1^0$ one expects a mass resolution of $\delta m_{\tilde{\chi}_1^{\pm}} = 0.2 \text{ GeV}$, while the di-jet mass distributions constrains the $\tilde{\chi}_1^{\pm} - \tilde{\chi}_1^0$ mass splitting to about 100 MeV. Similarly, the di-lepton energy and mass distributions in the reaction $e^+ e^- \rightarrow \tilde{\chi}_2^0 \tilde{\chi}_2^0 \rightarrow 4\ell^{\pm} \cancel{E}$ can be used to determine $\tilde{\chi}_1^0$ and $\tilde{\chi}_2^0$ masses to about 2 per mil³¹. Higher resolution of order 100 MeV for $m_{\tilde{\chi}_2^0}$ can be obtained from a threshold scan of $e^+ e^- \rightarrow \tilde{\chi}_2^0 \tilde{\chi}_2^0$; heavier states $\tilde{\chi}_3^0$ and $\tilde{\chi}_4^0$, if accessible, can still be resolved with a resolution of a few hundred MeV.

3.2. Couplings and mixings

The L - R mixing for the third generation can be non-negligible due to the large Yukawa coupling making the $\tilde{\tau}$, \tilde{t} and \tilde{b} systems very interesting to study to determine their mixing and chiral quantum numbers. Likewise, we would like to determine the gaugino and higgsino composition of charginos and neutralinos. Equally important is to verify the SUSY mass relations and exact equality (at tree level) of gauge couplings and their supersymmetric Yukawas. For all these measurements the ability of having *both* beams, positrons and electrons, polarised turns to be crucial³², since for many measurements even 100% electron polarisation is insufficient.

The couplings and mixing angles can be extracted from production cross sections measured with polarized beams. For example, experimental analyses of stop quarks with small stop-neutralino mass difference, motivated by the stop-neutralino co-annihilation DM scenario, are very demanding. Nevertheless, the stop parameters can be determined precise enough, Fig. 5 (left), and precisions for the dark matter predictions comparable to that from direct WMAP measurements in the region down to mass differences $\sim \mathcal{O}(5 \text{ GeV})$ can be achieved³³.

The Yukawa couplings of scalar fermions can precisely be determined by measuring the production cross-sections with polarized beams. For example, in the electroweak sector, the relation between the hypercharge $U(1)_Y$ coupling g_1 and the $SU(2)_L$ coupling g_2 and the corresponding Yukawa couplings \hat{g}_1 and \hat{g}_2 can accu-

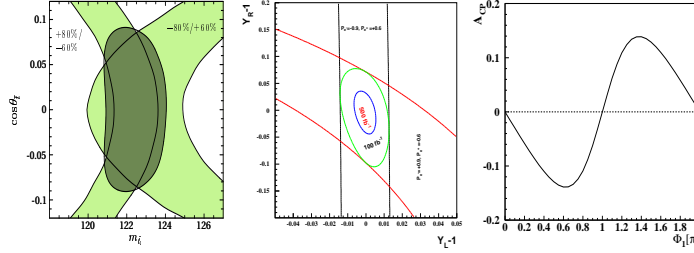


Fig. 5. Power of polarization – bounds on: (left) light stop mass $m_{\tilde{t}_1}$ and stop mixing angle $\theta_{\tilde{t}}$ from $\sigma(e^+e^- \rightarrow \tilde{t}_1 \tilde{t}_1^*)$; (center) on $Y_L = \hat{g}_2/g_2$ and $Y_R = \hat{g}_1/g_1$ from neutralino pair-production with polarized beams. (right) Φ_1 dependence of the CP-odd asymmetry A_{CP} .

rately be checked in neutralino pair-production. Combining the measurements of σ_R and σ_L for the process $e^+e^- \rightarrow \tilde{\chi}_1^0 \tilde{\chi}_2^0$, the Yukawa couplings can be determined to quite a high precision, as demonstrated in Fig. 5 (center)³⁴.

Polarisation is a very powerful tool not only for preparing the desirable initial state, but also as a diagnosis tool of final states. For example, neutralinos $\tilde{\chi}_2^0$ produced in \tilde{e}_L^\pm decays are 100% polarized³⁵. Furthermore, in $e^+e^- \rightarrow \tilde{e}_L^+ \tilde{e}_L^- \rightarrow e^+ \tilde{\chi}_1^0 e^- \tilde{\chi}_2^0$ followed by the three-body decay $\tilde{\chi}_2^0 \rightarrow \tilde{\chi}_1^0 \mu^+ \mu^-$ it is possible to reconstruct the rest frame of the neutralino $\tilde{\chi}_2^0$ as shown in Ref.³⁶. Such a perfect neutralino polarization combined with the study of angular correlations in the neutralino rest frame can provide us with ways for probing the Majorana nature of the neutralinos and CP violation in the neutralino system. With the neutralino spin vector \hat{n} and two final lepton momentum directions \hat{q}^+ and \hat{q}^- the CP-odd asymmetry can be constructed by comparing number of events with $O_{CP} = \hat{n} \cdot (\hat{q}_+ \times \hat{q}_-)$ positive and negative, normalized to the sum. Fig. 5 (right) shows the dependence of the CP-odd asymmetry on the phase Φ_1 of the bino mass parameter M_1 ³⁷.

3.3. Looking beyond the ILC kinematic reach

The precision measurements offered by the ILC allow us to infer indirect information on heavy states not directly accessible. As an illustration we consider two examples.

The first example concerns an interesting scenarios in which scalar particle sector is heavy while the gaugino masses are kept relatively small, like in the cosmology-motivated focus-point scenario³⁸. Precision analyses of cross sections for light chargino production and forward-backward asymmetries of decay leptons at the first stage of the ILC, Fig. 6 (left), together with mass information on $\tilde{\chi}_2^0$ and squarks from the LHC, show that the underlying fundamental gaugino/higgsino MSSM parameters and constrains on the heavy, kinematically inaccessible sparticles with masses $\mathcal{O}(2 \text{ TeV})$, can be obtained nevertheless³⁹.

If the second top squark \tilde{t}_2 is too heavy for the ILC, and due to huge background invisible at the LHC, the precise measurement of the Higgs boson mass m_h at ILC together with measurements from the LHC can be used to obtain indirect limits on $m_{\tilde{t}_2}$ ⁴⁰, Fig. 6. Both examples again demonstrate the power of the LHC/ILC

10 Jan Kalinowski

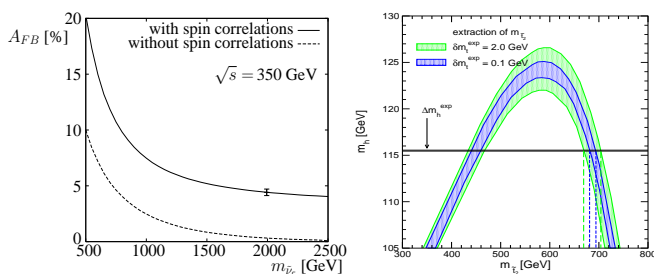


Fig. 6. Indirect determination of: $m_{\tilde{\nu}_e}$ from the forward-backward asymmetry of e^- in the process $e^+e^- \rightarrow \tilde{\chi}_1^+\tilde{\chi}_1^-$, $\tilde{\chi}_1^- \rightarrow \tilde{\chi}_1^0\ell^-\bar{\nu}$ (left); $m_{\tilde{t}_2}$ from the m_h measurement (right).

interplay, since neither of these colliders alone can provide sufficient data needed to determine the SUSY parameters in such difficult scenarios.

3.4. e^-e^- , $e\gamma$ and $\gamma\gamma$ options

Compton back-scattering of the laser light on electron beam(s) opens a possibility of converting the e^-e^- collider to an $e\gamma$ and $\gamma\gamma$ collider with energies and luminosities comparable to those of e^+e^- collider⁴¹. If realized, these options may open new discovery channels. Again I will take two specific examples to illustrate the point.

If the mass difference between the lightest neutralino and the selectron is a few hundred GeV, it may happen that chargino pair production at the ILC is possible, while selectron pair production is kinematically forbidden. However, $m_{\tilde{\chi}_1^0} + m_{\tilde{e}}$ can still be below 90% of the centre-of-mass energy, so that the process $e\gamma \rightarrow \tilde{\chi}_1^0\tilde{e}^-$ is possible at an $e\gamma$ collider. If the photon energy were known, the selectron and neutralino masses could be determined from the endpoints of the decay electron distribution, like in e^+e^- collisions. Although the variable photon energy smears the endpoints, simulations have shown (Fig. 7) that with the $m_{\tilde{\chi}_1^0}$ determined in e^+e^- running, the selectron mass can be reconstructed from the position of the lower edge⁴².

$\gamma\gamma$ collider offers a unique possibility of producing as s -channel resonances neutral Higgs bosons H, A that are *both* too heavy to be produced in associated HA or ZH processes at e^+e^- collider and lay in the so called ‘‘LHC-wedge’’ of intermediate values of $\tan\beta$, to which the LHC is blind. Results of a simulation for the combined $\gamma\gamma \rightarrow H, A \rightarrow b\bar{b}$ analyses are shown in Fig. 7⁴³ (the H and A bosons are almost mass-degenerate). Other decay modes ($WW, ZZ, t\bar{t}$) can provide a means to determine the Higgs-boson CP properties⁴⁴, and the τ -fusion process, $\gamma\gamma \rightarrow \tau\tau H, A$, can serve to measure $\tan\beta$ ⁴⁵, the parameter that is notoriously difficult to determine experimentally.

3.5. Beyond the ILC

It is expected that higher energy colliders will be needed to help unravel the multi-TeV physics left unveiled either by the LHC or by the ILC. Further progress in particle physics may require clean experiments at a linear e^+e^- collider at multi-TeV energies, like CLIC⁴⁶, which would be an ideal machine to complement the

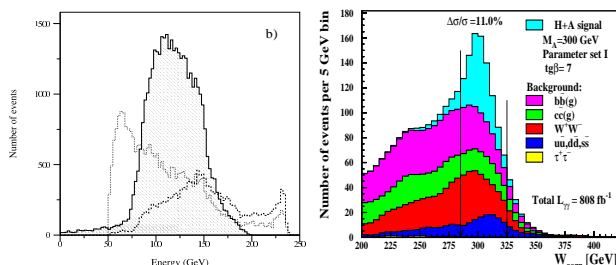


Fig. 7. Electron energy distribution signal $e\gamma \rightarrow \nu_e \nu_e e$ (shaded) and background after cuts (left). Invariant mass distribution for $\gamma\gamma \rightarrow H, A \rightarrow b\bar{b}$ and background (right).

the LHC and ILC physics program. Simulations for CLIC concentrated on such scenarios with particles beyond the LHC and ILC reach.

Fig. 8 (left) shows simulations of the muon energy spectrum from a 1150 GeV selectron decaying to a muon and a 660 GeV LSP neutralino. The endpoints are clearly seen allowing the selectron and neutralino mass determination. Likewise, in Fig. 8(middle) the di-muon invariant mass distribution from $\tilde{\chi}_2^0 \rightarrow \mu^+ \mu^- \tilde{\chi}_1^0$ exhibits a pronounced edge which, together with results from selectron decay make a measurement of $m_{\tilde{\chi}_2^0}$ possible.

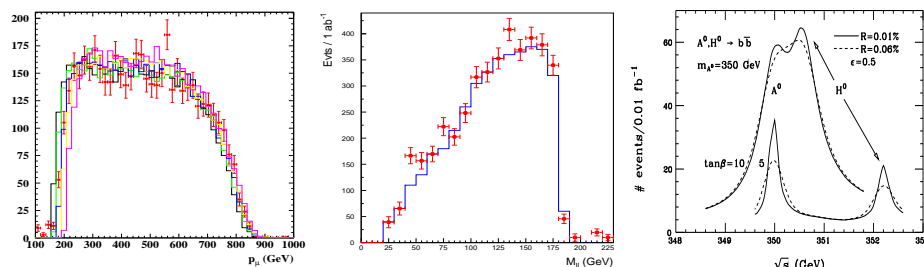


Fig. 8. Muon energy spectrum from $\tilde{\mu}_L \rightarrow \mu \tilde{\chi}_1^0$ (left), and di-muon invariant mass spectrum from $\tilde{\chi}_2^0 \rightarrow \mu^+ \mu^- \tilde{\chi}_1^0$ (middle) at CLIC. Separation of A and H signals at a muon collider (right).

In more distant future a muon collider with extremely good beam energy resolution will provide a tool to explore Higgs (and Higgs-like objects) by direct s -channel fusion because of enhanced couplings of muons to Higgs bosons, much like the LEP explored the Z . Right panel of Fig. 8 demonstrates how well two almost mass-degenerate Higgs bosons H and A can be resolved ⁴⁷.

4. Reconstructing the underlying SUSY model

The expected high experimental accuracies at the LHC/ILC could not be fully exploited if not matched from the theoretical side. This calls for a well defined theoretical framework for the calculational schemes in perturbation theory as well as for the input parameters. Motivated by the experience in analyzing data at the former e^+e^- colliders LEP and SLC, and building on vast experience in SUSY calculations and data simulations and analyses, the Supersymmetry Parameter Analysis

(SPA) Convention and Project¹¹ has been proposed. It recommends a convention for high-precision theoretical calculations, and provides a program repository of numerical codes, a list of tasks needed further improvements and a SUSY reference point SPS1a' as a test-bed.

The SPA Convention and Project is a joint inter-regional effort that could serve as a forum to discuss future improvements on both experimental and theoretical sides to exploit fully the physics potential of LHC, and ILC. The current status of the project is documented on the web-page <http://spa.desy.de/spa/>

4.1. SPA Convention

The SPA Convention consists of the following propositions:

- The masses of the SUSY particles and Higgs bosons are defined as pole masses.
- All SUSY Lagrangian parameters, mass parameters and couplings, including $\tan\beta$, are given in the \overline{DR} scheme at the scale $\tilde{M} = 1$ TeV.
- Gaugino/higgsino and scalar mass matrices, rotation matrices and the corresponding angles are defined in the \overline{DR} scheme at \tilde{M} , except for the Higgs system in which the mixing matrix is defined in the on-shell scheme, the scale parameter chosen as the light Higgs mass.
- The Standard Model input parameters of the gauge sector are chosen as G_F , α , M_Z and $\alpha_s^{\overline{MS}}(M_Z)$. All lepton masses are defined on-shell. The t quark mass is defined on-shell; the b , c quark masses are introduced in \overline{MS} at the scale of the masses themselves while taken at a renormalization scale of 2 GeV for the light u , d , s quarks.
- Decay widths, branching ratios and production cross sections are calculated for the set of parameters specified above.

4.2. Program repository

The repository contains links to codes grouped in several categories: scheme translation tools; spectrum calculators from the Lagrangian parameters; calculators of various observables: decay tables, cross sections, low-energy observables, cold dark matter relics, cross sections for CDM particle searches; event generators; analysis programs to extract the Lagrangian parameters from experimental data; RGE codes; as well as some auxiliary programs and libraries.

The responsibility for developing codes and maintaining them up to the current theoretical state-of-the-art precision rests with the authors. The SLHA⁴⁸ convention is recommended for communication between the codes.

4.3. The test-bed: Ref. Point SPS1a'

To perform first checks of its internal consistency and to explore the potential of such coherent data analyses a MSSM Reference Point SPS1a' has been proposed as a

testing ground. The roots defining SPS1a' are the mSUGRA parameters $M_{1/2} = 250$ GeV, $M_0 = 70$ GeV, $A_0 = -300$ GeV at the GUT scale, and $\tan\beta(\tilde{M}) = 10$, $\mu > 0$. The point is close to the original Snowmass point SPS1a²⁸ and to point B' of ⁴⁹. Recently global analysis programs have become available ⁵⁰ in which the whole set of data, masses, cross sections, branching ratios *etc.*, is exploited coherently to extract the Lagrangian parameters in the optimal way after including the available radiative corrections.

The parameter set SPS1a' chosen for a first study provides a benchmark for developing and testing the tools needed for a successful analysis of future SUSY data. However, neither this specific point nor the MSSM itself may be the correct model for low-scale SUSY. Other scenarios might be realized in the SUSY sector and the SPA convention is general enough to cover them.

Although current SPA studies are very encouraging, much additional work both on the theoretical as well as on the experimental side will be needed to achieve the SPA goals.

5. Summary

Much progress has been achieved in preparing the physics programme for new machines. At the beginning the LHC has been considered merely as a discovery machine. However, over the years many techniques have been developed for extracting masses and couplings, and in some cases the Lagrangian parameters. Many experimental analyses are still based on lowest-order expressions. On the theory side many higher-order calculations have been completed and implemented in numerical codes. New theoretical ideas deserve experimental analyses. However, the task of exploring all masses and couplings of SUSY particles is probably impossible by the LHC alone. The ILC will extend the discovery reach, in particular in the electroweak sector, and greatly improve on precision SUSY measurements. We still need new ideas and techniques to explore fully the opportunities offered to us by the LHC and ILC. The SPA Convention and Project should prove very useful in streamlining discussions and comparisons of different calculations and experimental analyses.

Acknowledgment

I would like to thank the organizers and Dr. Khalil Shaban in particular for hospitality and creative atmosphere at the conference. Work supported by the Polish Ministry of Science and Higher Education Grant No 1 P03B 108 30.

References

1. ALEPH, DELPHI, L3, OPAL and SLD Collaborations and LEPEW, SLDEW and SLD Heavy Flavour Working Groups, *Precision electroweak measurements on the Z resonance*, Phys. Rept. **427** (2006) 257. See also talk of J. D. Lykken, these Proceedings [arXiv:hep-ph/0609274].
2. Yu. A. Golfand and E. P. Likhtman, JETP Lett. **13** (1971) 323 [Pisma Zh. Eksp.

- Teor. Fiz. **13** (1971) 452]. D. V. Volkov and V. P. Akulov, JETP Lett. **16** (1972) 438 [Pisma Zh. Eksp. Teor. Fiz. **16** (1972) 621]. J. Wess and B. Zumino, Phys. Lett. B **49** (1974) 52.
3. \protect\vrule width0pt\protect\href{http://www-cdf.fnal.gov/physics/exotic/exotic.html}{http://www-cdf.fnal.gov/physics/exotic/exotic.html}\protect\vrule width0pt\protect\href{http://www-d0.fnal.gov/Run2Physics/WWW/results/np.html}{http://www-d0.fnal.gov/Run2Physics/WWW/results/np.html}\protect\vrule width0pt\protect\href{http://www-h1.desy.de/h1/www/publications/H1_sci_results.shtml}{http://www-h1.desy.de/h1/www/publications/H1_sci_results.shtml}\protect\vrule width0pt\protect\href{http://www-zeus.desy.de/publications.php3}{http://www-zeus.desy.de/publications.php3}
 4. ATLAS Collab., *ATLAS Detector and physics performance technical design report*, CERN-LHCC-99-14/15 (1999).
 5. CMS Collab., *CMS Physics Technical Design Report*, CERN-LHCC-2006-021 (2006).
 6. M. L. Mangano, M. Moretti, F. Piccinini, R. Pittau and A. D. Polosa, JHEP **0307** (2003) 001. T. Plehn, D. Rainwater and P. Skands, Phys. Lett. B **645**, 217 (2007) [arXiv:hep-ph/0510144]. S. Asai, talk at 4th TEV4LHV, Oct. 20-22, 2005.
 7. S. Kachru, R. Kallosh, A. Linde and S. P. Trivedi, Phys. Rev. D **68** (2003) 046005.
 8. K. Choi, K. S. Jeong and K. i. Okumura, JHEP **0509** (2005) 039. A. Falkowski, O. Lebedev and Y. Mambrini, JHEP **0511** (2005) 034.
 9. K. Kawagoe and M. M. Nojiri, Phys. Rev. D **74**, 115011 (2006) [arXiv:hep-ph/0606104].
 10. I. Hinchliffe et al., Phys. Rev. D **55** (1997) 5520.
 11. J. A. Aguilar-Saavedra *et al.*, Eur. Phys. J. C **46** (2006) 43. See also J. Kalinowski, Supersymmetry Parameter Analysis, *Proc. Int. Conference on Supersymmetry and Unification of Fundamental Interactions SUSY02 (Hamburg 2002)*, arXiv:hep-ph/0212388.
 12. B. K. Gjelsten, D. J. Miller and P. Osland, JHEP **0412** (2004) 003.
 13. M. M. Nojiri, G. Polesello and D. R. Tovey, JHEP **0603** (2006) 063.
 14. E. A. Baltz, M. Battaglia, M. E. Peskin and T. Wizansky, Phys. Rev. D **74** (2006) 103521 [arXiv:hep-ph/0602187].
 15. K. Desch, J. Kalinowski, G. Moortgat-Pick, M. M. Nojiri and G. Polesello, JHEP **0402** (2004) 035.
 16. M. M. Nojiri, G. Polesello and D. R. Tovey, arXiv:hep-ph/0312317. K. Kawagoe, M. M. Nojiri and G. Polesello, Phys. Rev. D **71** (2005) 035008.
 17. H. C. Cheng, K. T. Matchev and M. Schmaltz, Phys. Rev. D **66** (2002) 056006.
 18. A. J. Barr, Phys. Lett. B **596** (2004) 205.
 19. J. M. Smillie and B. R. Webber, JHEP **0510** (2005) 069.
 20. C. Athanasiou, C. G. Lester, J. M. Smillie and B. R. Webber, JHEP **0608** (2006) 055. L. T. Wang and I. Yavin, JHEP **0704**, 032 (2007) [arXiv:hep-ph/0605296].
 21. P. M. Zerwas *et al.*, arXiv:hep-ph/0211076. C. G. Lester, M. A. Parker and M. J. White, JHEP **0601** (2006) 080 [arXiv:hep-ph/0508143].
 22. N. Arkani-Hamed, G. L. Kane, J. Thaler and L. T. Wang, JHEP **0608** (2006) 070.
 23. J.A. Aguilar-Saavedra *et al.*, TESLA Technical Design Report, DESY 01-011 and arXiv:hep-ph/0106315; T. Abe *et al.* [American LC WG], in *Proceedings of the APS/DPF/DPB Summer Study on the Future of Particle Physics (Snowmass 2001)*, SLAC-R-570 and arXiv:hep-ex/0106055-58; T. Abe *et al.* [Asian LC WG], KEK-Report-2001-011 and arXiv: hep-ph/0109166.
 24. G. Weiglein *et al.* [LHC/LC Study Group], Phys. Rept. **426**, 47 (2006) [arXiv:hep-ph/0410364].
 25. \protect\vrule width0pt\protect\href{http://www.linearcollider.org}{http://www.linearcollider.org}
 26. Int. Linear Collider Reference Design Report 2007 [ILC-REPORT-2007-001], ²⁵.
 27. \protect\vrule width0pt\protect\href{http://www.desy.de/conferences/ecfa-lc-study.html}{http://www.desy.de/conferences/ecfa-lc-study.html}\protect\vrule width0pt\protect\href{http://acfahep.kek.jp}{http://acfahep.kek.jp}\protect\vrule width0pt\protect\href{http://physics.uoregon.edu/string~lc/alcpag}{http://physics.uoregon.edu/string~lc/alcpag}

28. B. C. Allanach *et al.*, Eur. Phys. J. C **25** (2002) 113.
29. A. Freitas *et al.*, arXiv:hep-ph/0211108. A. Freitas, Ph.D. thesis, Hamburg (2002), DESY THESIS-2002-023.
30. H. U. Martyn, arXiv:hep-ph/0406123.
31. H. U. Martyn, arXiv:hep-ph/0302024.
32. G. A. Moortgat-Pick *et al.*, arXiv:hep-ph/0507011.
33. M. Carena, A. Finch, A. Freitas, C. Milstene, H. Nowak and A. Sopczak, Phys. Rev. D **72** (2005) 115008.
34. S. Y. Choi, J. Kalinowski, G. A. Moortgat-Pick and P. M. Zerwas, Eur. Phys. J. C **22** (2001) 563 [Addendum-ibid. C **23** (2002) 769].
35. J.A. Aguilar-Saavedra, Phys. Lett. B **596** (2004) 247.
36. J.A. Aguilar-Saavedra and A.M. Teixeira, Nucl. Phys. B **675** (2003) 70. J.A. Aguilar-Saavedra, LC-TH-2003-098 [hep-ph/0312140].
37. S. Y. Choi, B. C. Chung, J. Kalinowski, Y. G. Kim and K. Rolbiecki, Eur. Phys. J. C **46** (2006) 511.
38. J. L. Feng, K. T. Matchev and T. Moroi, Phys. Rev. D **61** (2000) 075005. J. L. Feng and F. Wilczek, Phys. Lett. B **631** (2005) 170.
39. K. Desch, J. Kalinowski, G. Moortgat-Pick, K. Rolbiecki and W. J. Stirling, JHEP **0612**, 007 (2006) [arXiv:hep-ph/0607104].
40. S. Heinemeyer, S. Kraml, W. Porod and G. Weiglein, JHEP **0309** (2003) 075.
41. For a review and references see e.g. V. I. Telnov, Acta Phys. Polon. B **37** (2006) 1049.
42. I. Alvarez Illan and K. Monig, DESY LC note LC-PHSM-2005-002.
43. P. Niezurawski, A. F. Zarnecki and M. Krawczyk, Acta Phys. Polon. B **37** (2006) 1187;
44. P. Niezurawski, A. F. Zarnecki and M. Krawczyk, Acta Phys. Polon. B **36** (2005) 833. S. Y. Choi, J. Kalinowski, Y. Liao and P. M. Zerwas, Eur. Phys. J. C **40** (2005) 555 [arXiv:hep-ph/0407347], and arXiv:hep-ph/0508121.
45. S. Y. Choi *et al.*, Phys. Lett. B **606** (2005) 164.
46. E. Accomando *et al.* [CLIC Physics Working Group], arXiv:hep-ph/0412251.
47. M. M. Alsharoa *et al.* [Muon Collider/Neutrino Factory Collaboration], Phys. Rev. ST Accel. Beams **6** (2003) 081001.
48. P. Skands *et al.*, JHEP **0407** (2004) 036.
49. M. Battaglia *et al.*, Eur. Phys. J. C **33** (2004) 273.
50. P. Bechtle, K. Desch and P. Wienemann, Comput. Phys. Commun. **174** (2006) 47. R. Lafaye, T. Plehn and D. Zerwas, arXiv:hep-ph/0404282.